Supplementary data

ASXL2 regulates hematopoiesis in mice and its deficiency promotes myeloid expansion

Supplementary Methods

Genomic DNA extraction

Genomic DNA was extracted from BM mononuclear cells using a DNA extraction kit (Puregene Gentra System, Minneapolis, MN, USA) according to the manufacturer's instructions. Genomic DNA was quantified using Qubit Fluorometer (Life Technologies) and DNA integrity was assessed by agarose gel electrophoresis. For samples with low quantity, DNA was amplified using REPLI-g Ultrafast mini kit (Qiagen).

Peripheral blood analysis

Complete peripheral blood counts were analysed using Abbott Cell-Dyn 3700 hematology analyzer (Abbott Laboratories).

Expression analysis of Asxl2 and Asxl1

Transcript levels of Asxl2 and Asxl1 were estimated using quantitative RT-PCR with following primers: Asxl2 primer set 1, ATTCGACAAGAGATTGAGAAGGAG (forward) and TTTCTGTGAATCTTCAAGGCTTAG (reverse); Asxl2 primer set 2, GCCCTTAACAATGAGTTCTTCACT (forward) and TCCACAGCTCTACTTTCTTCTCCT (reverse); Asxl1 primers, GGTGGAACAATGGAAGGAAA (forward) and CTGGCCGAGAACGTTTCTTA (reverse). Asxl2 protein was detected in immunoblot using anti-ASXL2 antibody (Bethyl).

In vitro differentiation of bone marrow cells

Bone marrow (BM) cells were cultured in IMDM containing 20% FBS and 10 ng/ml IL3, 10 ng/ml IL6, 20 ng/ml SCF and 20 ng/ml GMCSF for two weeks. For FACS analysis, cells were washed, stained with fluorochrome-conjugated antibodies and analysed on FACS LSR II flow cytometer (BD Biosciences) using FACSDIVA software (BD Biosciences).

Colony re-plating assay

Bone marrow cells were plated in methylcellulose medium containing mouse stem cell factor (SCF), mouse interleukin 3 (IL-3), human interleukin 6 (IL-6) and human erythropoietin (MethoCult GF M3434; StemCell Technologies). Colonies were enumerated after 9-12 days and cells were harvested for re-plating.

BrdU incorporation assay

Mice were injected intraperitoneally with bromodeoxyuridine (BrdU) (1 mg BrdU/mouse) and euthanized 2 hours later. Bone marrow cells were harvested from femurs and tibias, Lin^- cells were enriched using Dynabeads Sheep anti-rat IgG and stained with fluorochrome-conjuagted antibodies. Cells were then fixed and permeabilized using APC BrdU Flow Kit (BD Biosciences) as per the manufacturer's instruction and stained with anti-BrdU antibody and Hoechst 33342 dye (1 μg/ml). Samples were acquired on LSRII flow cytometer (BD Biosciences) and data were analysed using FACSDIVA software (BD Biosciences).

Myeloperoxidase staining

Spleens were fixed with 10% formalin for 24 hours and embedded in paraffin. Four μm thick sections were cut, paraffin was removed using xylene and sections were rehydrated with ethanol. Endogenous peroxidase activity was blocked with 3% hydrogen peroxide in methanol for 10 min. Heat-induced antigen retrieval was performed in 0.01M Citrate buffer, pH 6.0 at 95°C for 25 min. The slides were then stained with rabbit polyclonal Myeloperoxidase (Agilent, A039829-2) for 45 min at room temperature. The signal was detected using Dako EnVision+ System (Agilent, K4003). All sections were visualized with the diaminobenzidine reaction and counterstained with hematoxylin.

Competitive and non-competitive reconstitution assay

For competitive repopulation assay, $Lin^{-}Kit^{+}Sca1^{+}$ (LSK) cells sorted from the *Asxl2* KO or WT mice (expressing CD45.2) were mixed with LSK cells from the competitor B6.SJL-Ptprca Pepcb/BoyJ (B6.SJL) strain (expressing CD45.1). 2,000 or 4,000 total LSK cells were injected in the tail vein of lethally irradiated (11 Gy) recipient mice (B6.SJL x 129 F1) (expressing both CD45.1 and CD45.2). Recipient mice also received 500,000 spleen cells harvested from non-irradiated mice (B6.SJL x 129 F1). Following transplantation, peripheral blood was collected from the facial vein every four weeks, red cells were lysed using ACK solution, and leukocytes were stained with antibodies against CD45.1, CD45.2 and the lymphoid (CD3 and CD19) and myeloid (CD11b, Gr1 and F4/80) cells. Donor contribution to different lineages was analyzed on FACS LSR II using FACSDIVA software (BD Biosciences). For non-competitive reconstitution assay, two million bone marrow cells from either WT or *Asxl2* KO mice were injected intravenously in lethally irradiated mice. Engraftment was assessed after 4 weeks, mice were euthanized one year after transplantation, and lymphoid organs were analyzed using flow cytometry.

Flow cytometry

Single cell suspensions from bone marrow, spleen and thymus were incubated with fluorochrome-conjugated antibodies for 30 min on ice. Cells were washed with 2% FBS/PBS and resuspended in SYTOX Blue Dead Cell Stain (ThermoFisher Scientific) (1:10,000 dilution in 2% FBS/PBS). Cells were acquired on FACS LSR II flow cytometer (BD Biosciences) and data were analyzed using FACSDIVA software (BD Biosciences). Sorting of cells was performed on FACSAria cell sorter (BD Biosciences). See Supplementary Table S2 for the list of antibodies used for flow cytometric staining.

RNA sequencing and expression analysis

RNA was extracted from FACS-sorted LSK cells from *Asxl2* KO and WT littermates using Qiagen RNeasy Micro Kit. cDNA libraries were prepared from poly-A selected RNA using SMART-Seq v4 Ultra Low Input RNA Kit (Clontech Laboratories; Mountain View, CA, USA). For BM cells expressing mutant or wild-type ASXL2, RNA was extracted using Qiagen RNeasy Mini Kit and libraries prepared using TruSeq sample preparation kit (Illumina). Libraries were sequenced on HiSeq 4000 and 100 bp paired-end reads were aligned to mouse reference transcriptome (GRCm38/mm10; Ensemble version 84) using Kallisto (version 0.43.0).[1] Transcript level fragment counts were summarized to gene level using TxImport Bioconductor package and differential analysis was performed using DESeq2.[2, 3] Gene expression was quantified in FPKM units using DESeq2 fpkm command and was used for all downstream analysis and plotting. All other test-statistics and plotting were performed using R 3.4.0. Gene Ontology (GO) was performed on differentially expressed genes using goseq Bioconductor package (version 1.20.0), which accounts for bias due to gene length.2 Resulting p-values were adjusted for False Discovery Rate (FDR). For GSEA analysis we used all “active transcripts” with mean expression of 0.5 FPKM to identify significantly enriched gene sets among MSigDB C2 gene sets.[4] Genes were rank ordered according to their fold change between WT and KO mice, as determined by mean number of RNA-Seq reads across two replicates per condition.

Supplementary References

1. Bray NL, Pimentel H, Melsted P, Pachter L. Near-optimal probabilistic RNA-seq quantification. Nat Biotechnol. 2016;34(5):525-527.
2. Soneson C, Love MI, Robinson MD. Differential analyses for RNA-seq: transcript-level estimates improve gene-level inferences. F1000Res. 2015;4(1521.

3. Love MI, Huber W, Anders S. Moderated estimation of fold change and dispersion for RNA-seq data with DESeq2. Genome Biol. 2014;15(12):550.
4. Subramanian A, Tamayo P, Mootha VK, et al. Gene set enrichment analysis: a knowledge-based approach for interpreting genome-wide expression profiles. Proc Natl Acad Sci U S A. 2005;102(43):15545-15550.

Supplementary Figure S1

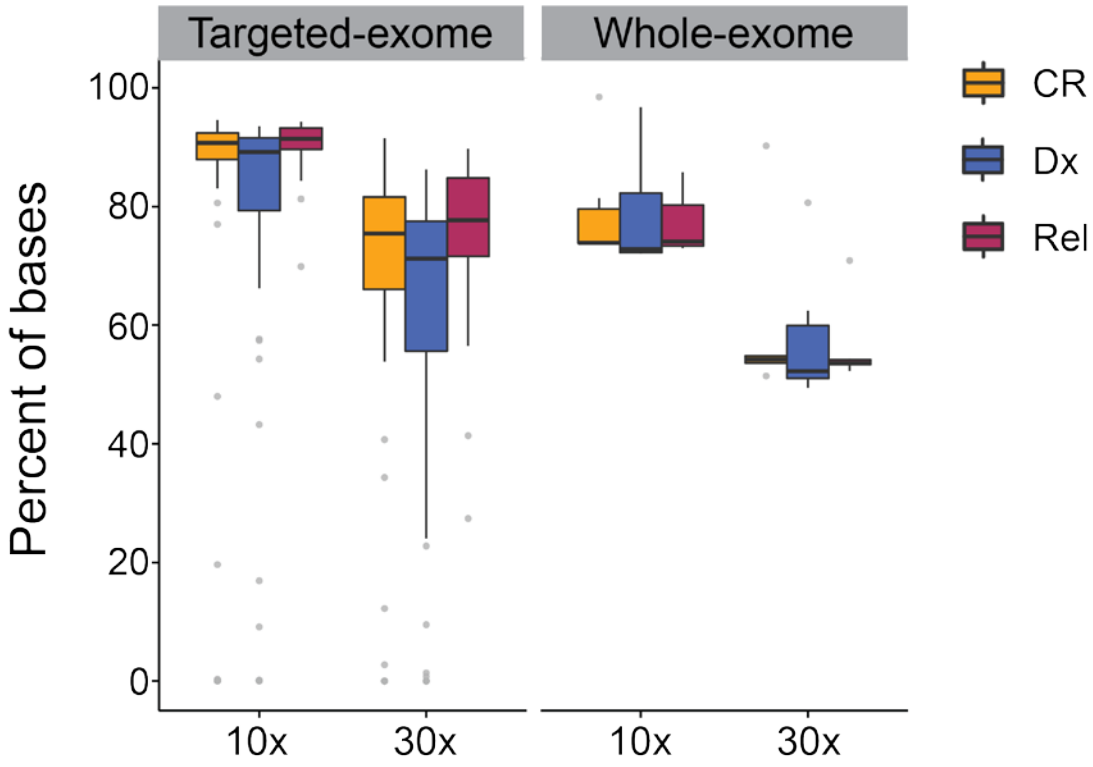

Supplementary Figure S1: Sequencing coverage of t(8;21) AML samples analysed by whole exome and targeted exome sequencing. Box plots show proportion of bases covered at 10x and 30x sequencing depth for diagnosis (Dx), relapse (Rel) and complete remission (CR) samples.

Supplementary Figure S2

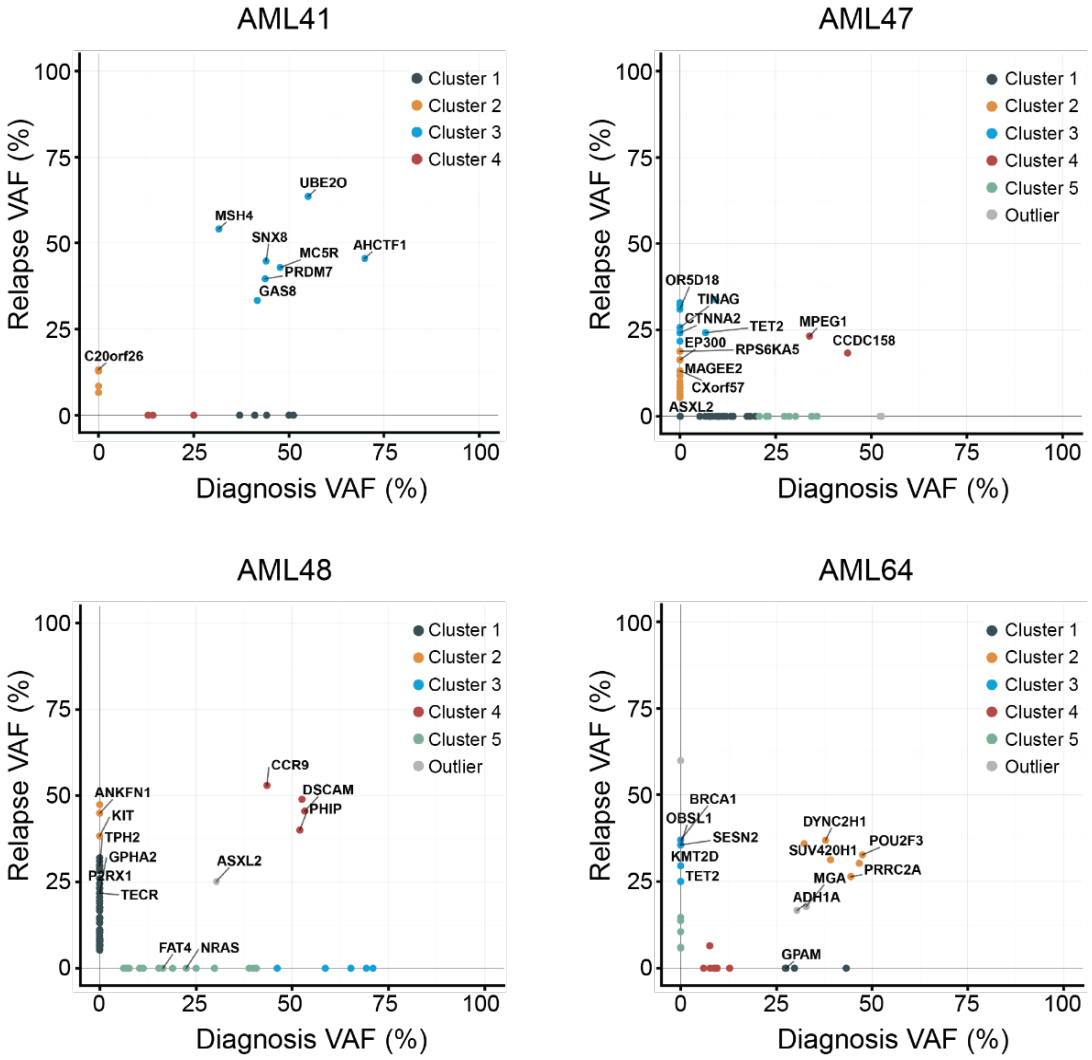

Supplementary Figure S2: Representative plots depict variant allele frequencies (VAF) of somatic mutations identified at diagnosis and relapse in four t(8;21) AML cases analysed using whole exome sequencing.

Supplementary Figure S3

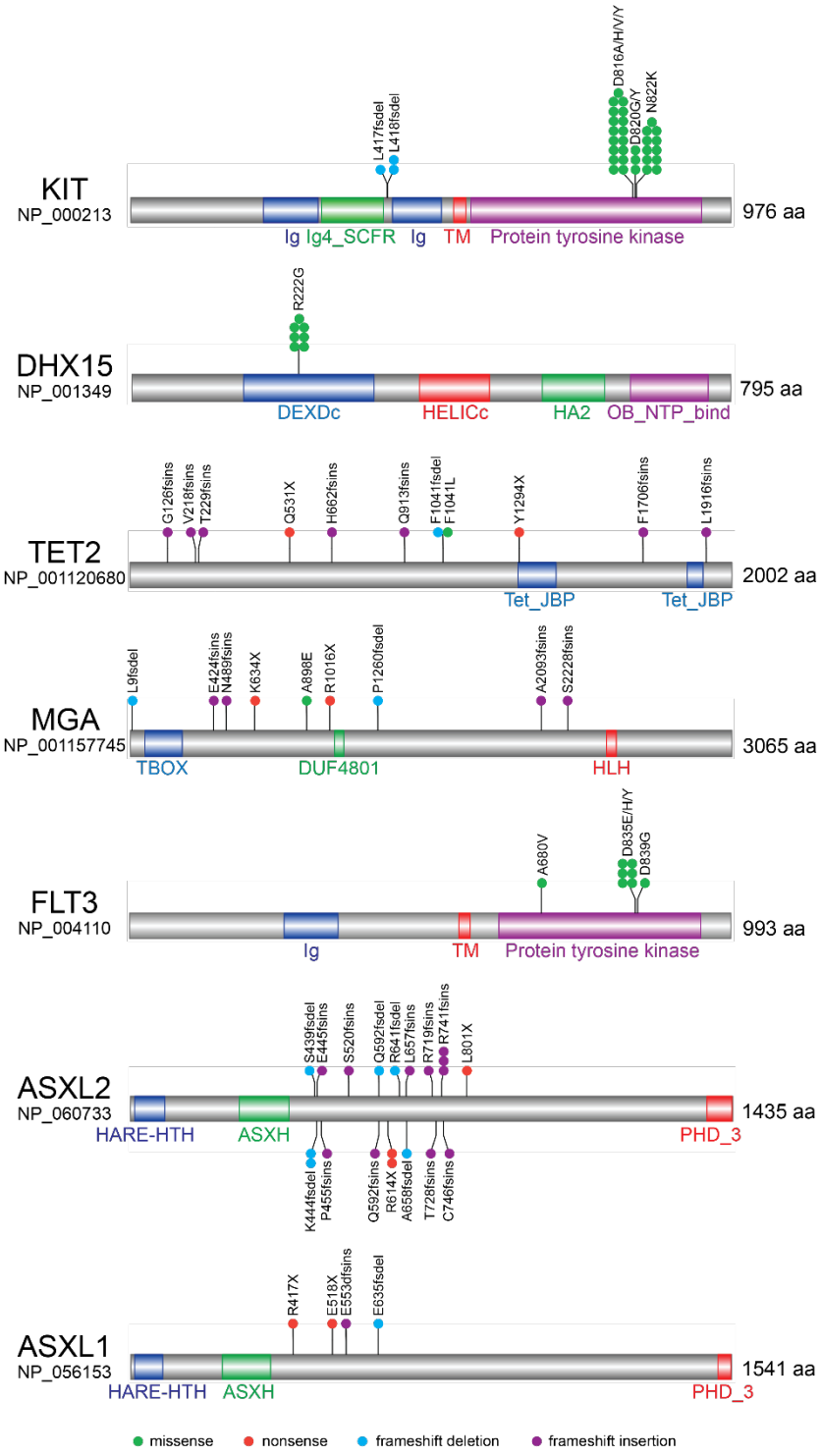

Supplementary Figure S3: Schematic representation of protein domains of frequently mutated genes in our t(8;21) AML cohort are shown along with location and type of somatic mutations. Illustrations were prepared with IBS software using the motif information from NCBI Protein database (http://www.ncbi.nlm.nih.gov/protein). Circles depicting individual mutations are color coded for different types of mutations. For matched primary and relapse samples, mutations that are detected at both stages

are depicted only once. Ig: Immunoglobulin domain, Ig4_SCFR: Fourth immunoglobulin (Ig)-like domain of stem cell factor receptor, TM: transmembrane region, DEXDc: DEAD-like helicases superfamily, HELICc: helicase superfamily c-terminal domain, HA2=Helicase associated domain, OB_NTP_bind: Oligonucleotide/oligosaccharide-binding (OB)-fold, Tet_JBP: Oxygenase domain of the 2OGFeDO superfamily, TBOX: T-box DNA binding domain of the T-box family of transcriptional regulators, DUF4801: Domain of unknown function, HLH: Helix-loop-helix DNA-binding domain, HARE-HTH: HB1, ASXL, restriction endonuclease HTH domain, ASXH: Asx homology domain and PHD_3: PHD domain of transcriptional enhancer, Asx.

Supplementary Figure S4

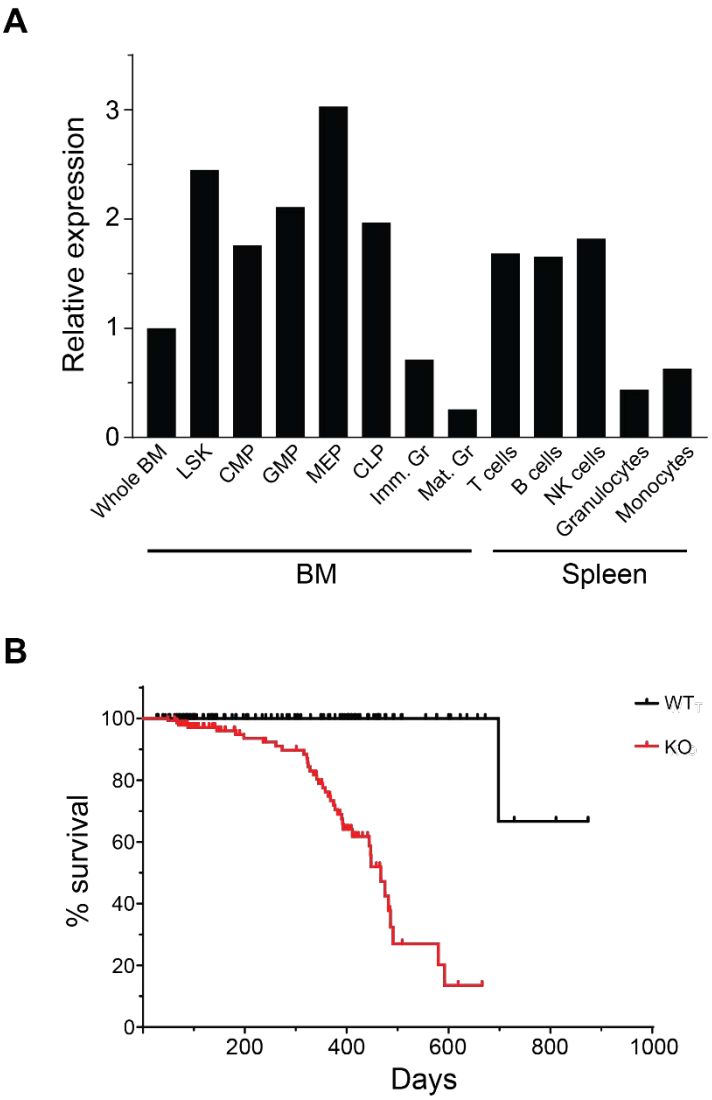

Supplementary Figure S4: (A) *Asxl2* transcript levels in different hematopoietic cells sorted from either bone marrow or spleen of C57BL/6 mice. Imm. Gr: Immature granulocytes ($CD11b^{+}Gr1^{inter}$), Mat. Gr: Mature granulocytes ($CD11b^{+}Gr1^{hi}$). (B) Kaplan Meier curve depicts the survival duration of WT (n=207) and *Asxl2* KO (n=145) mice ($p<0.0001$, Log-rank (Mantel-Cox) test).

Supplementary Figure S5

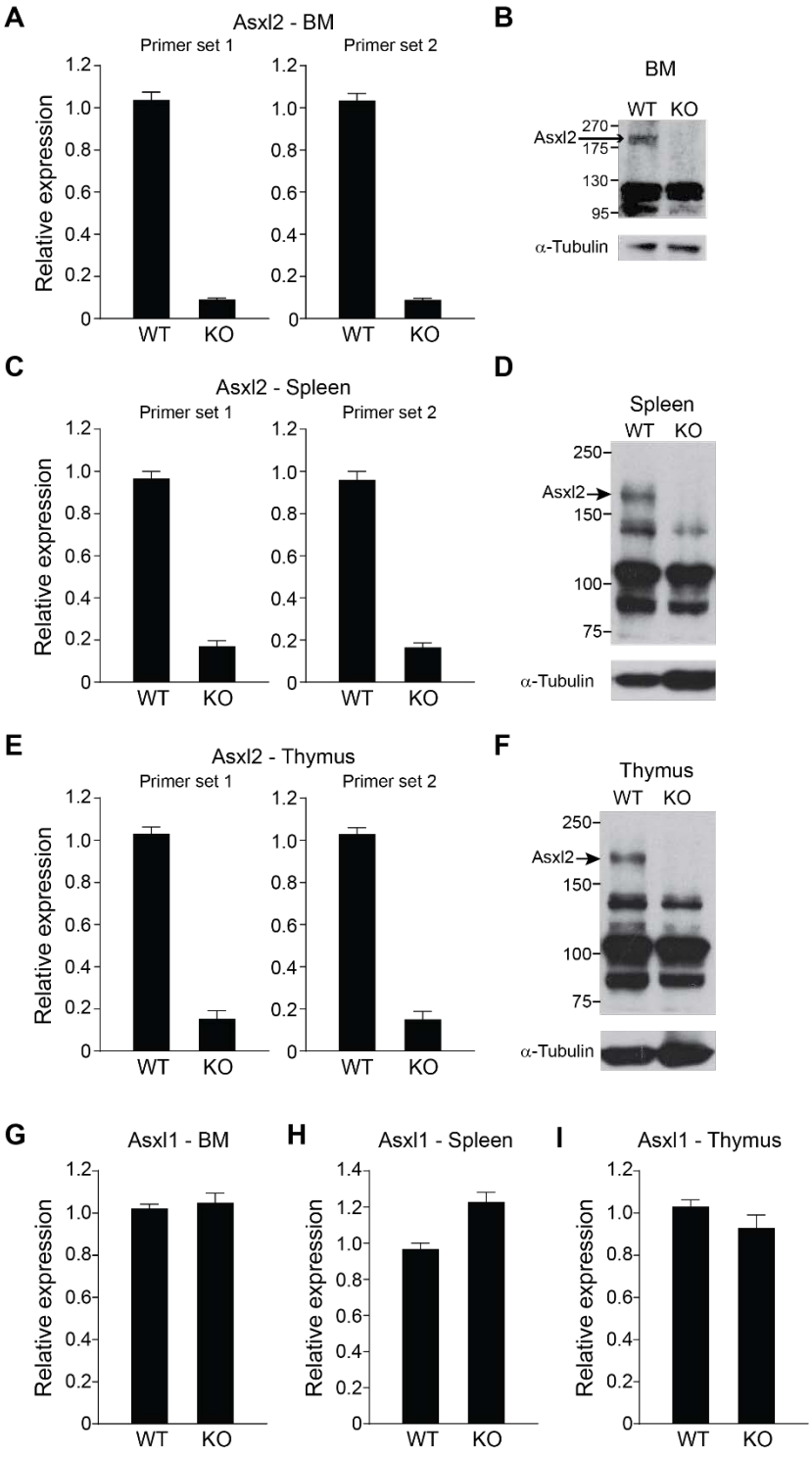

Supplementary Figure S5: (A-F) Significantly reduced transcript and protein levels of Asxl2 in in the bone marrow (BM) (A-B), spleen (C-D) and thymus (E-F) of *Asxl2* gene-trap (KO) mice compared with the WT mice. (G-I) Transcript levels of *Asxl1* in bone marrow (G), spleen (H) and thymus (I) of WT and *Asxl2* gene-trap (KO) mice. Bars represent mean ± SEM.

Supplementary Figure S6

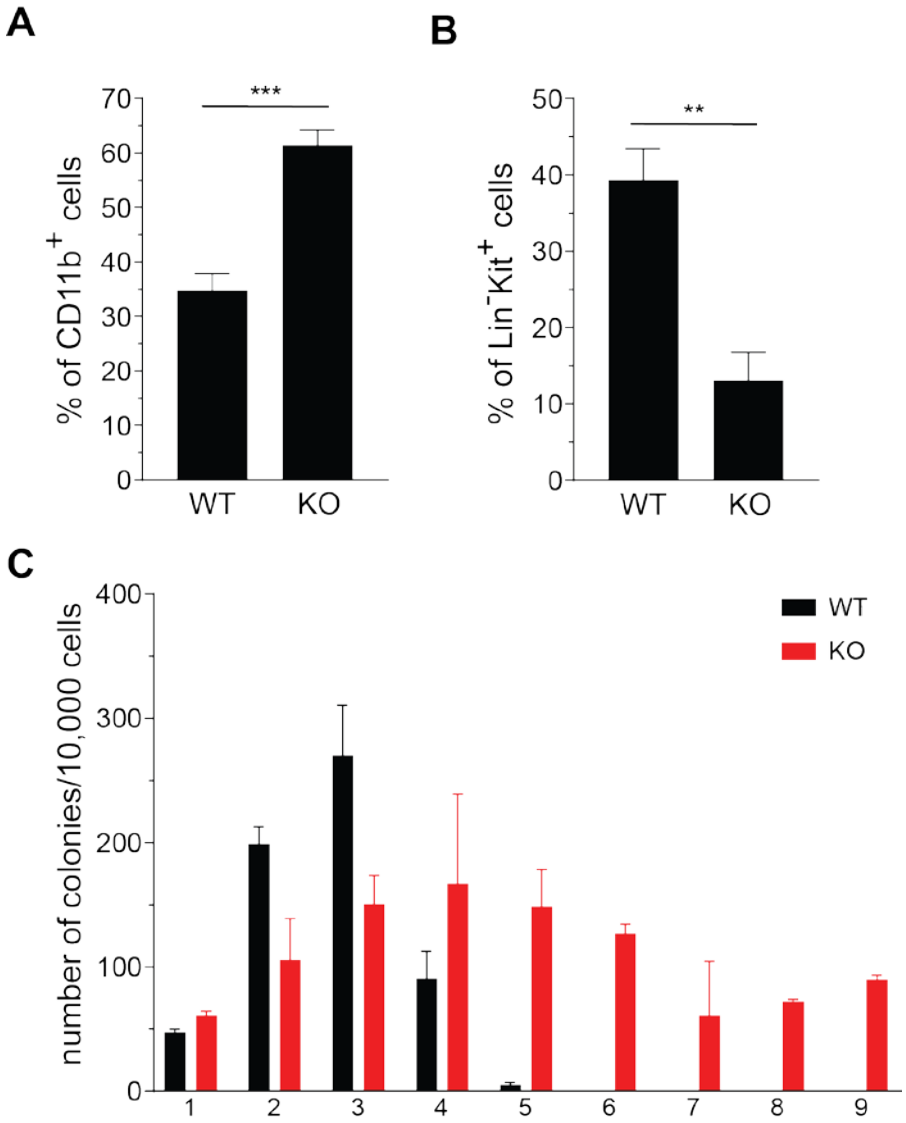

Supplementary Figure S6: (A-B) Proportion of $CD11b^+$ (A) and Lin^-Kit^+ cells (B) identified using flow cytometry in *in vitro* differentiation of *Asxl2* WT and KO BM cells. Cells were cultured in the presence of IL3, IL6, SCF and GMCSF for two weeks (n=8 for WT; n=4 for KO). (C) Colony re-plating assay using *Asxl2* WT and KO BM cells. Cells were plated in duplicate and colonies were enumerated after 9-12 days (n=5 for WT; n=3 for KO). Data are represented as mean ± SEM. ** p<0.01, *** p<0.001.

Supplementary Figure S7

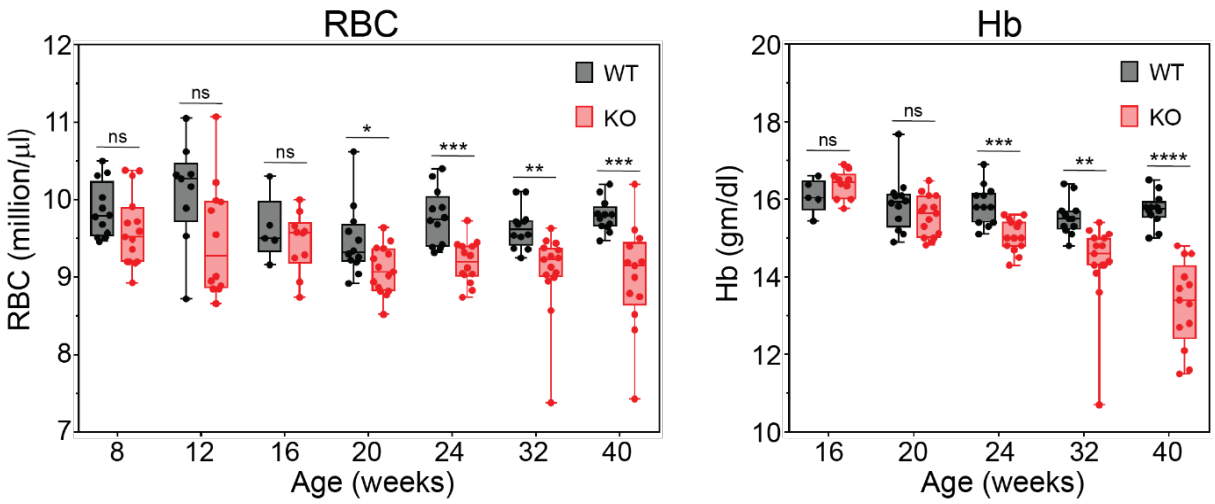

Supplementary Figure S7: Periodic analysis of RBC counts and hemoglobin (Hb) levels in peripheral blood of WT and *Asxl2* deficient mice. Whiskers extend from the smallest to the largest values**.** *p <0.05, **p<0.01, ***p<0.001, ****p<0.0001, ns = not significant.

Supplementary Figure S8

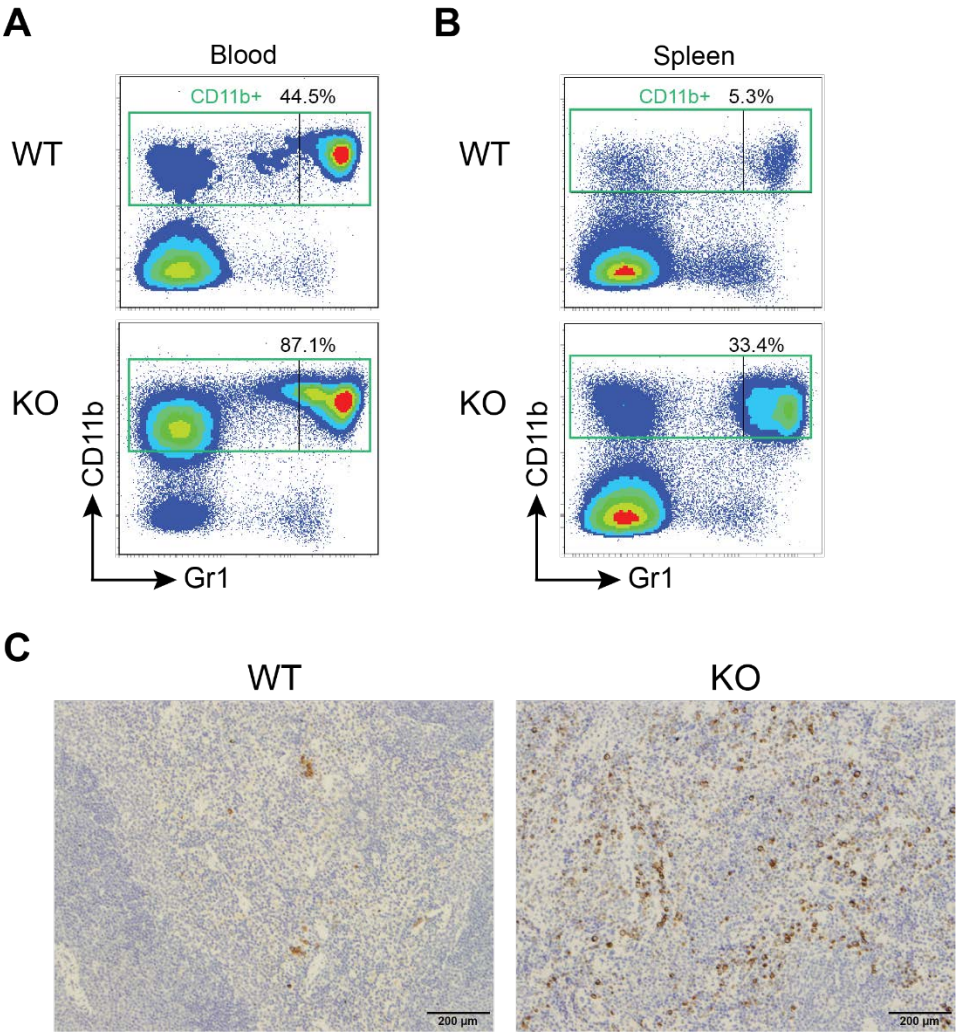

Supplementary Figure S8: (A-B) Representative FACS plots depict proportion of mature myeloid cells in the peripheral blood (A) and spleen (B) of >1-year old WT and *Asxl2* KO mice. (C) Representative photographs of immunohistochemical staining for myeloperoxidase in sections of spleens from >1-year old WT and *Asxl2* KO mice (10x objective using Olympus IX71 microscope).

Supplementary Figure S9

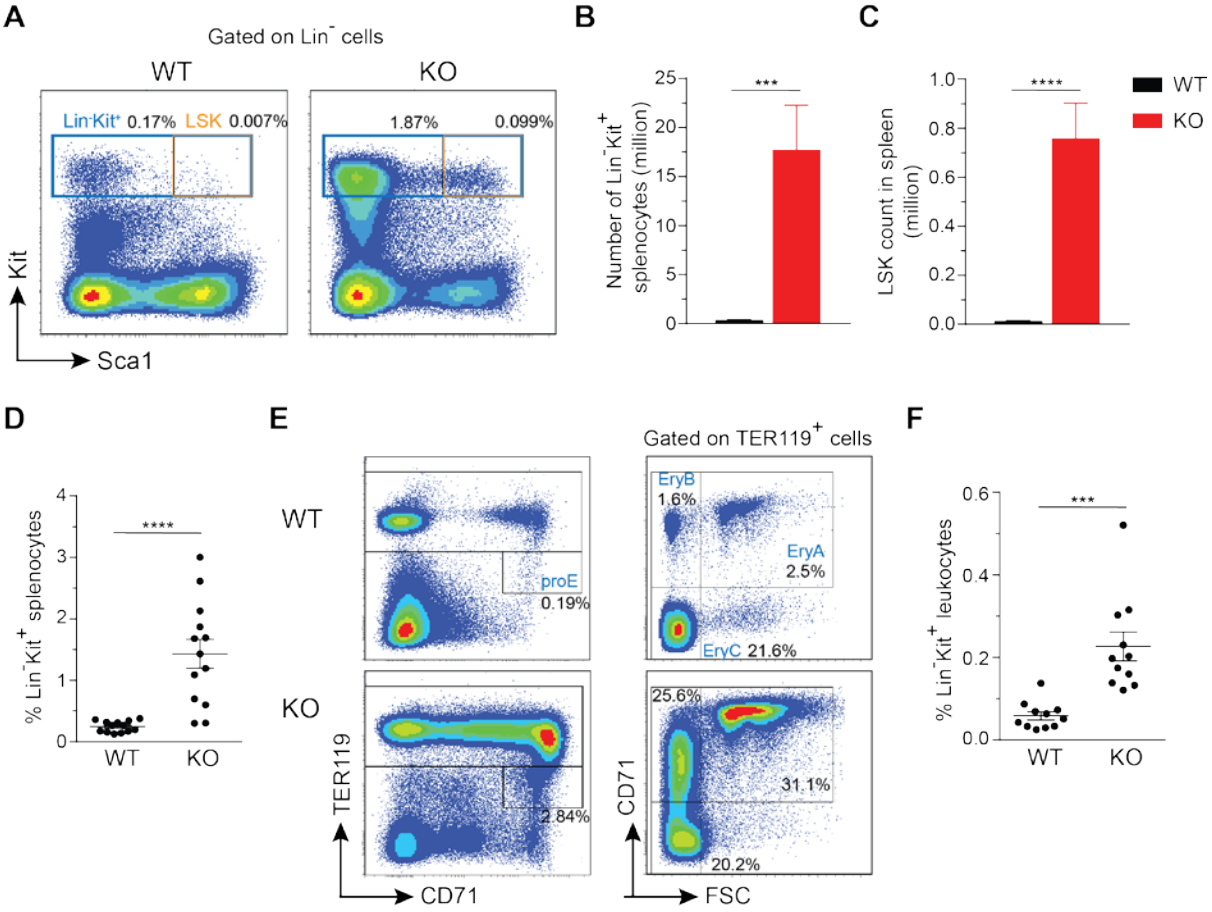

Supplementary Figure S9: (A) Density plots depict representative staining for LSK and total Lin$^-$Kit$^+$ populations in spleens of >1-year old WT and *Asxl2* KO mice. (B-C) Absolute numbers of Lin$^-$Kit$^+$ (B) and LSK (C) cells in the spleen of old WT and *Asxl2* KO mice (n=13). (D) Proportion of Lin$^-$Kit$^+$ cells in the spleen of old WT and *Asxl2* KO mice. (E) Representative FACS plots show successive stages of erythroid cell maturation (proE → EryA → EryB → EryC) using antibodies against CD71 and TER119 in the spleen of >1-year old mice. (F) Percentage of Lin$^-$Kit$^+$ cells in nucleated peripheral blood cells of >1-year old WT and *Asxl2* KO mice are depicted. Data are represented as mean ± SEM. ***p<0.001, ****p<0.0001.

Supplementary Figure S10

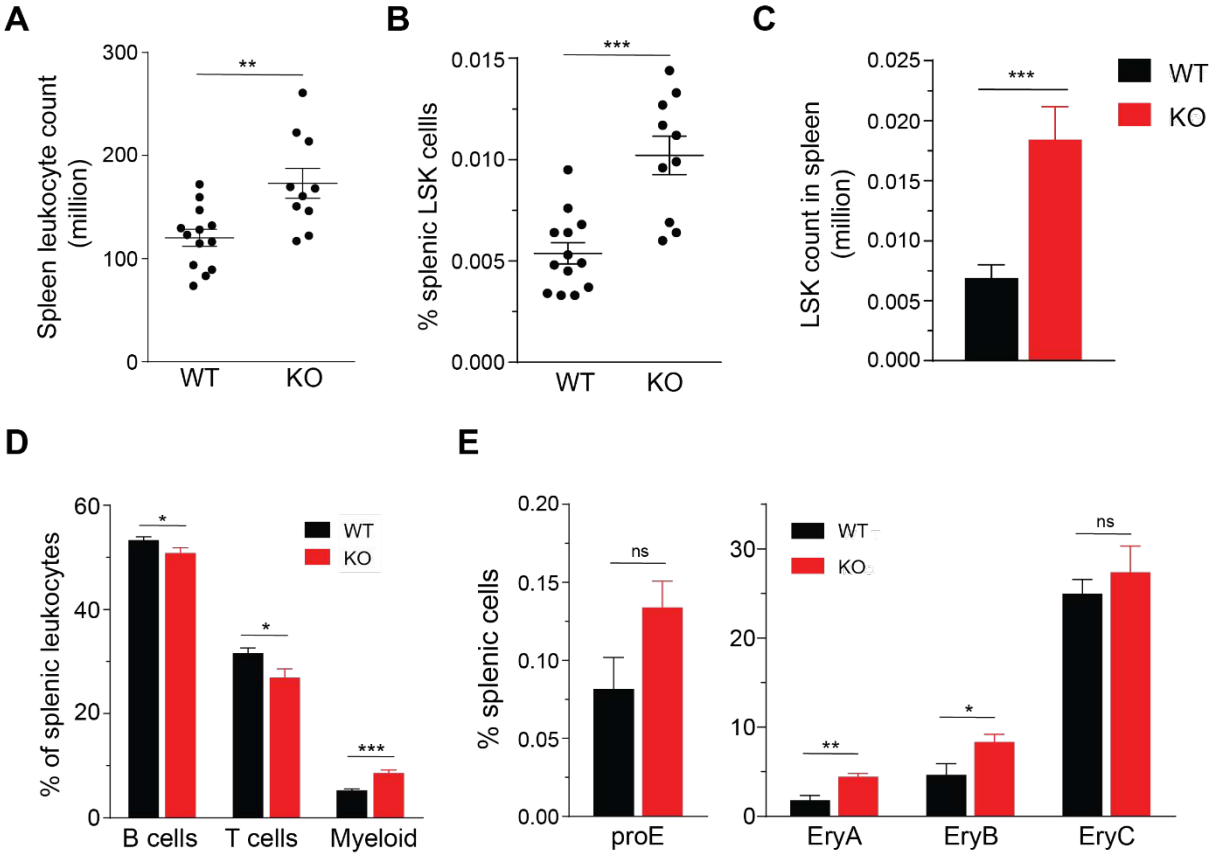

Supplementary Figure S10: (A) Spleen cellularity in 8-14 weeks old WT and *Asxl2* KO mice. (B-C) Proportion (B) and absolute number (C) of LSK cells in the spleen of young (8-14 weeks old) WT and *Asxl2* KO mice (n=13 for WT; n=10 for KO). (D) Percentages of B ($CD19^+$), T ($CD3^+$) and myeloid ($CD11b^+$) cells in the spleen of young (8-14 weeks old) WT and *Asxl2* KO mice (n=10-14 for WT; n=7-11 for KO). (E) Frequency of erythroid precursors in the spleen of young mice as determined by flow cytometric analysis using anti-CD71 and anti-TER119 antibodies (n=8). Data are represented as mean ± SEM. *p <0.05, **p<0.01, ***p<0.001, ns = not significant.

Supplementary Figure S11

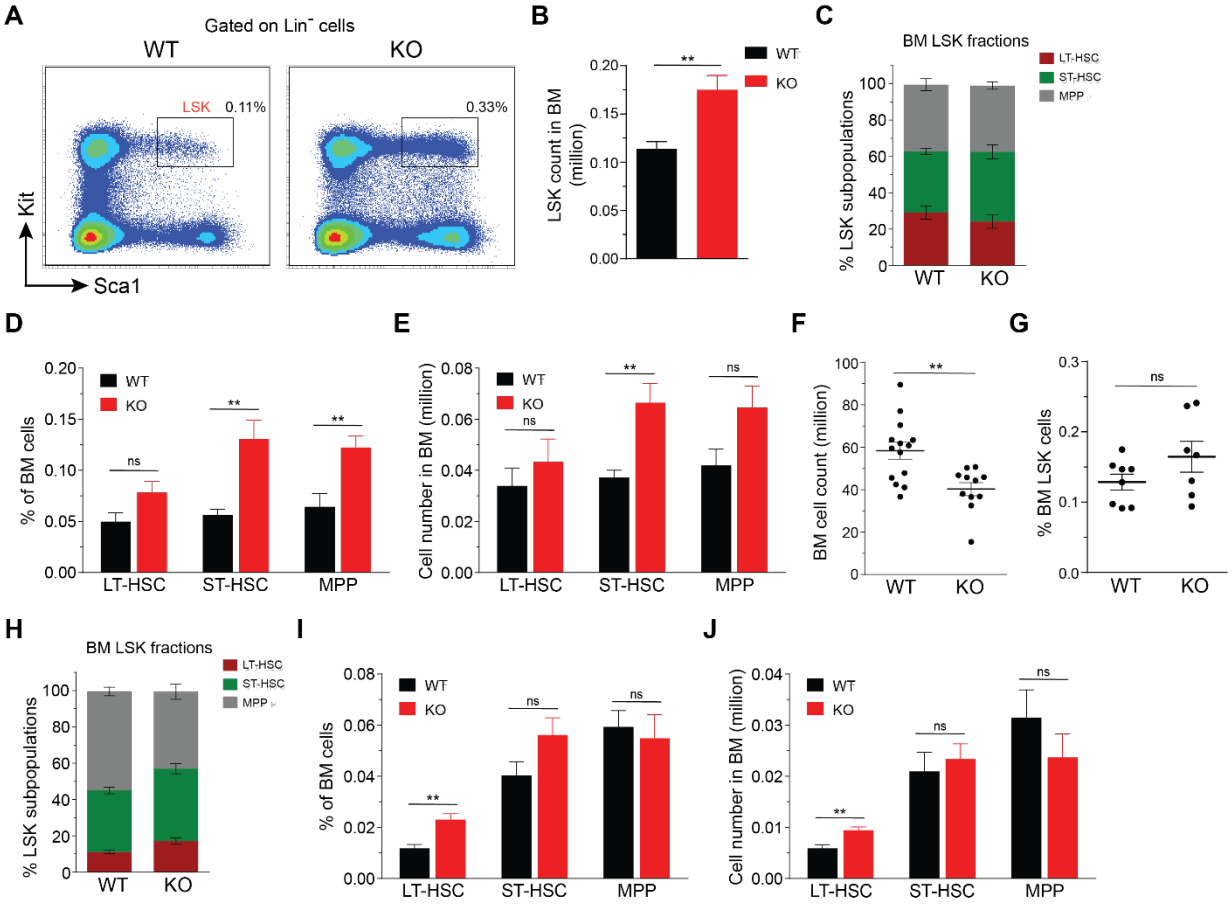

Supplementary Figure S11: (A) Representative FACS plots depict LSK population in >1-year old WT and *Asxl2* KO mice. (B) Absolute number of LSK cells in the bone marrow (two femurs + two tibias) of old mice (n=14). (C) Relative proportions of long term HSCs (LT-HSCs) ($CD34^{-}Flt3^{-}LSK$), short-term HSCs (ST-HSCs) ($CD34^{+}Flt3^{-}LSK$) and multipotent progenitors (MPPs) ($CD34^{+}Flt3^{+}LSK$) subpopulations within the LSK compartment in the BM of the old mice. (D) Frequencies of LT-HSCs, ST-HSCs and MPPs in the BM of >1-year old WT and KO mice. (E) Absolute numbers of LT-HSCs, ST-HSCs and MPPs in the BM of >1-year old WT and KO mice. (F) Bone marrow cellularity (two femurs + two tibias) in 8-14 weeks old WT and *Asxl2* KO mice. (G) Frequency of LSK cells in the bone marrow of young mice. (H) Relative proportions of LT-HSCs, ST-HSCs and MPPs subpopulations within the LSK compartment in the BM of the young mice. (I) Frequencies of LT-HSCs, ST-HSCs and MPPs in the BM of 8-14 weeks old WT and KO mice. (J) Absolute numbers of LT-HSCs, ST-HSCs and MPPs in the BM of young WT and KO mice. Data are represented as mean ± SEM. ** $p<0.01$, ns = not significant.

Supplementary Figure S12

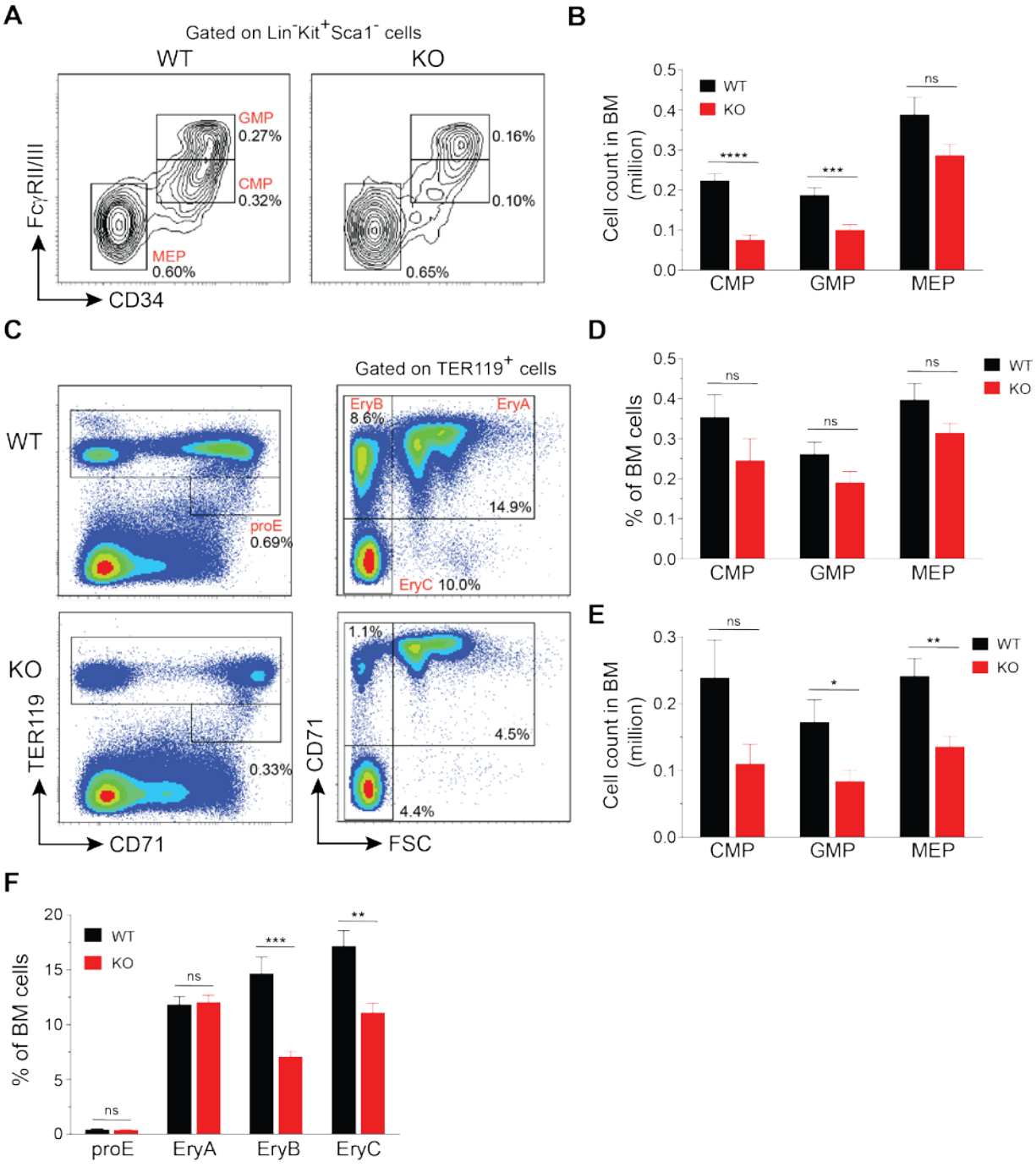

Supplementary Figure S12: (A) Representative contour plots depict flow cytometric staining for erythro-myeloid progenitors in the BM. Percentage of CMP, GMP and MEP cells in the bone marrow of old WT and KO mice are indicated. (B) Absolute cell counts for CMP, GMP and MEP populations in the bone marrow (two femurs + two tibias) of >1-year old mice (n=12). (C) Representative flow cytometry analysis for erythroid progenitors in the BM of >1-year old WT and KO mice. (D-E) Percentages (D) and absolute numbers (E) of CMP, GMP and MEP cells in the BM of 8-14 weeks old WT and *Asxl2* KO mice (n=7 for WT; n=6 for KO). (F) Frequency of cells in advancing

stages of erythroid differentiation in the BM of 8-14 weeks old WT and *Asxl2* KO mice (n=8 for WT; n=7 for KO). Bars represent mean ± SEM. *p <0.05, **p<0.01, ***p<0.001, ****p<0.0001, ns = not significant.

Supplementary Figure S13

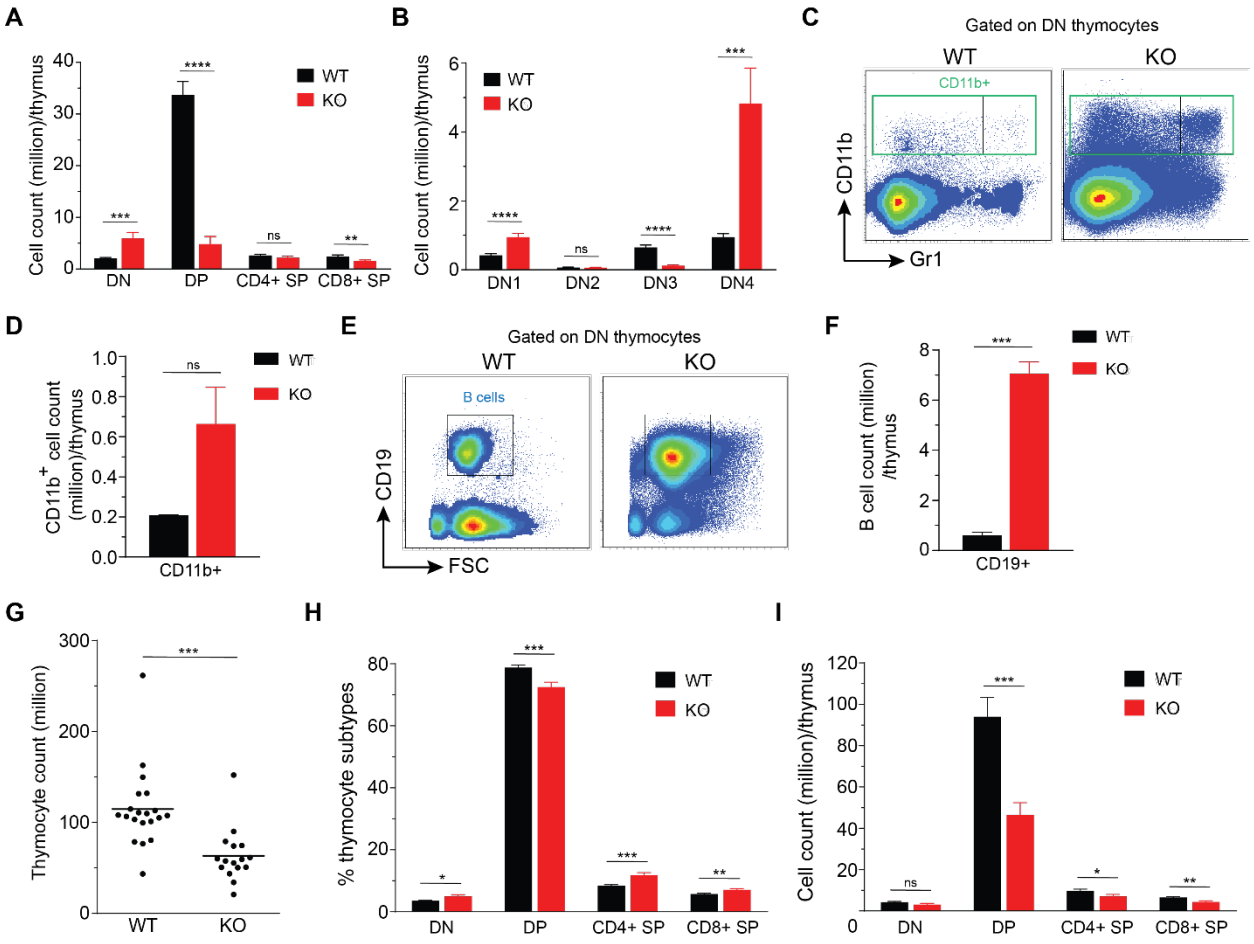

Supplementary Figure S13: (A) Absolute numbers of cells in the double negative (DN) ($CD4^-CD8^-$), double positive (DP) ($CD4^+CD8^+$), $CD4^+$ SP and $CD8^+$ SP compartments in the thymus of old WT and *Asxl2* KO mice are depicted (n=14 each). (B) Absolute number of cells in DN1, DN2, DN3 and DN4 compartment in the thymus of >1-year old WT and KO mice. (C) Density plots depict representative staining with anti-CD11b and anti-Gr1 antibodies within the DN compartment of >1-year old WT and KO mice. (D) Bars represent number of $CD11b^+$ cells in the thymus of old WT and KO mice. (E) Representative FACS plots for $CD19^+$ cells within the DN compartment of old WT and KO mice are shown. (F) Absolute number of B cells in the thymus of old WT and *Asxl2* KO mice (n=3). G) Thymus cellularity of young (8-14 weeks old) WT and *Asxl2* KO mice. (H-I) Frequency (H) and absolute number (I) of cells in DP, DN, $CD4^+$ SP and $CD8^+$ SP compartments in young WT and KO mice (n=17 (WT); n=15 (KO)). Data are represented as mean ± SEM. *p <0.05, **p<0.01, ***p<0.001, ****p<0.0001, ns = not significant.

Supplementary Figure S14

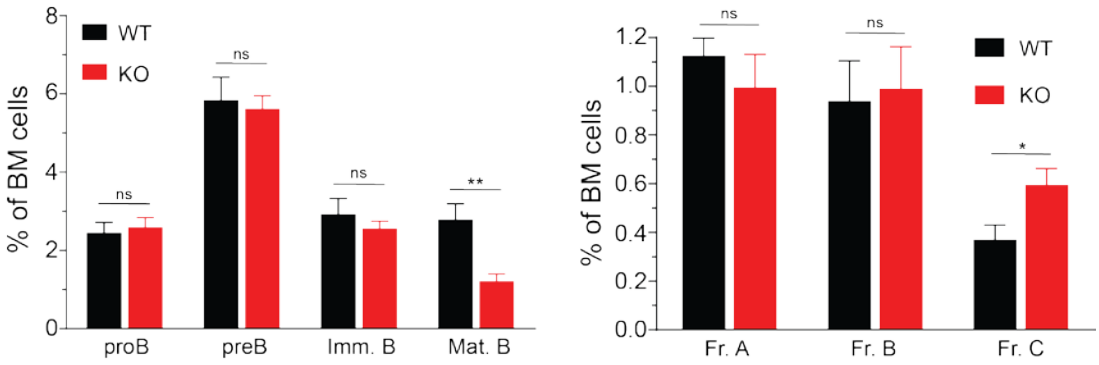

Supplementary Figure S14: Frequencies of B cell precursors in the bone marrow of young WT and *Asxl2* KO mice. proB: $CD43^{+}B220^{+}$, preB: $CD43^{-}B220^{+}IgM^{-}$, immature B (Imm. B): $CD43^{-}B220^{+}IgM^{+}$, mature B (Mat. B): $CD43^{-}B220^{hi}IgM^{+}$, Fraction A (Fr. A): $CD24^{-}BP1^{-}$ proB cells, Fraction B (Fr. B): $CD24^{+}BP1^{-}$ proB cells, Fraction C (Fr. C): $CD24^{+}BP1^{+}$ proB cells. Results are depicted as mean ± SEM. *p <0.05, ** p<0.01, ns = not significant.

Supplementary Figure S15

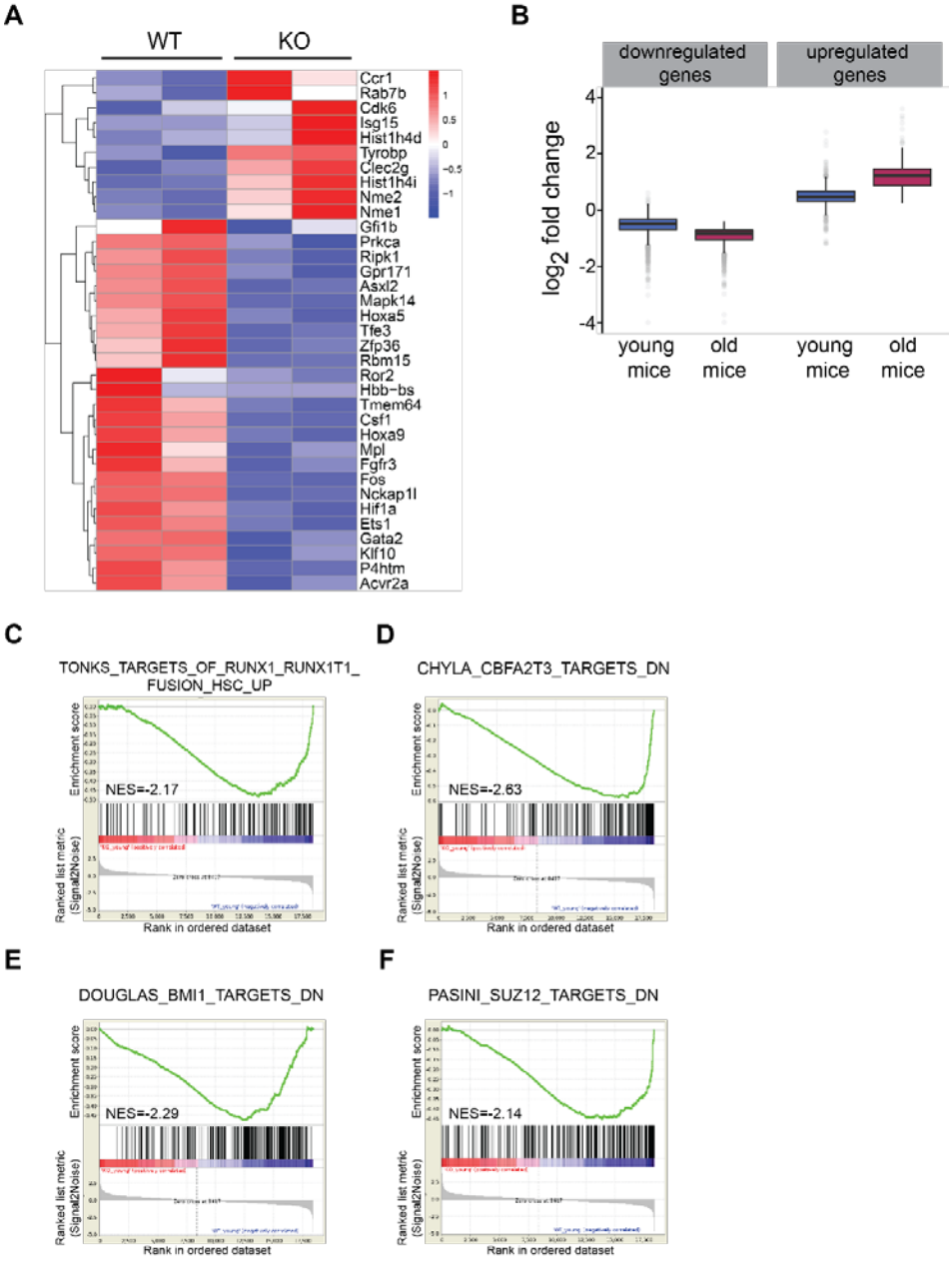

Supplementary Figure S15: (A) Heat map shows levels of differentially expressed genes (FDR<0.1) from Gene Ontology biological process 'regulation of myeloid cell differentiation genes' (GO:0045637) in the LSK cells from >1-year old *Asxl2* KO mice compared with the LSK cells from the old WT mice. (B) Box plots depict relative expression in LSK cells from young and old mice for genes either significantly downregulated or upregulated (FDR<0.1) in LSK cells from old mice. (C-D) GSEA plots of selected gene sets enriched in the LSK cells from young control and *Asxl2* KO littermates (corresponding to the plots in Figure 7D-E for the old mice). (E-F) GSEA plots for genes down-regulated in Ewing's sarcoma cell line upon knockdown of BMI1 (E), and genes down-regulated in SUZ12 deficient ES cells (F), in LSK cells from WT and KO littermates.

Supplementary Tables S1-S6

Supplementary Table S1: Genes analysed by targeted capture approach in frequency cohort of t(8;21) AML

Supplementary Table S2: Antibodies used for flow cytometric analysis

Supplementary Table S3: Clinical information for t(8;21) AML samples used for whole exome and targeted exome sequencing

Supplementary Table S4: Somatic mutations validated in whole exome sequencing of ten paired newly diagnosed and relapsed t(8;21) AML samples

Supplementary Table S5: Driver mutations identified in discovery and validation cohorts of t(8;21) AML

Supplementary Table S6: Differentially expressed genes in Asxl2 deficient LSK cells (old and young mice)

Separate excel files for Supplementary Tables S3-S6

Supplementary Table S1: Genes analysed by targeted capture approach in frequency cohort of t(8;21) AML

ABCA12	BRIP1	DAAM2	FBLN2	HYDIN	LTK	NOTCH3	PRAM1	SEMA6D	TINAG
ABL1	BTN3A3	DAPK1	FBXO34	ICA1L	LURAP1L	NOTCH4	PRDM15	SERPINB11	TMEM200B
ABL2	C10ORF118	DAXX	FBXO38	ID1	MAGEE2	NPDC1	PRDM7	SESN2	TMEM203
ACACB	C10ORF2	DCDC5	FBXW7	ID2	MAGI2	NPHS1	PRIC285	SET	TNRC6B
ADAMTSL3	C16ORF90	DCHS2	FCGBP	ID3	MAML1	NPM1	PROKR1	SETD1B	TNRC6C
ADCYAP1R1	C1ORF101	DDI2	FCN3	IDH1	MAP3K4	NR1H4	PRSS16	SF1	TOP1
ADH1A	C1ORF104	DDX10	FHIT	IDH2	MAP4K2	NRAS	PRSS3	SF3A1	TOP3B
ADORA1	C1QTNF7	DDX41	FLT3	IDH3B	MATN4	NSD1	PRUNE2	SF3B1	TPH2
ADSSL1	C22ORF31	DEK	FN1	IDO2	MC5R	NSDHL	PSD	SF3B2	TPSB2
AF15Q14	C8ORF80	DHX15	FNBP1	IGF2BP3	METTL13	NSMCE1	PSIP2	SGK2	TRIO
AGBL5	CACNA1E	DHX34	FREM2	IL10RA	MGA	NUP214	PSMD3	SGK3	TRIP11
AHCTF1	CASP1	DIRC2	FRG1B	IL7R	MKL1	NUP98	PTEN	SHANK1	TRPV2
AHNAK2	CBFA2T1	DIS3	FRG2C	INO80	MLF1	OBSL1	PTPN1	SHROOM2	TTK
AKAP12	CBFA2T3	DNAH9	GAS7	INSC	MLL	ODZ2	PTPN11	SIK3	TTN
ALAD	CBFB	DNAJB6	GAS8	IQSEC3	MLL2	OR14J1	PTPN13	SLA	U2AF1
ALDH5A1	CBL	DNAJC12	GATA1	ISM1	MLL3	OR1A2	PTPRB	SLC22A12	U2AF2
AMAC1L1	CBLB	DNMT1	GATA2	ISX	MN1	OR2T4	PUF60	SLC25A19	UBASH3A
ANKFN1	CBLC	DNMT3A	GATA3	ITPR1	MPEG1	OR8K3	PWWP2B	SLC34A1	UBE2O
ANKMY1	CCDC13	DOT1L	GBP4	JAK1	MPL	P2RX1	PXK	SLC6A9	USH2A
ANKRD20A4	CCDC83	DSCAM	GBP7	JAK2	MPRIP	P2RY2	PXN	SLC7A8	USP20
ANKRD24	CCR9	DSPP	GIGYF2	JAK3	MSF	PAM16	PYGO2	SLC9A2	USP31
ANKS4B	CDH13	DYNC1I2	GLTSCR1	JMJD5	MSH4	PAQR6	QRSL1	SLFN11	USP6
APC	CDH18	DYSF	GMPS	KCNG1	MSH6	PAQR9	RAD21	SMC1A	VCAN
APOB	CDH8	ECSIT	GNAS	KCNH6	MST1P9	PCDHA1	RAPGEF2	SMC3	VCPIP1
AR	CDT1	EED	GPAM	KCNH7	MST1R	PCDHGA1	RBM15	SMG1	VPS13C
ARHGAP6	CDX2	EFCAB5	GPBAR1	KDM5A	MT-CO2	PCDHGA2	RBM42	SMPDL3B	WAC
ARHGEF12	CEBP	EGFR	GPHA2	KDM5C	MT-CYB	PCDHGA3	RBMX	SNX12	WDR33
ARHGEF3	CEBPA	EIF2S3	GPR139	KDM6A	MTIF2	PCDHGA4	RELN	SNX8	WDR65
ARID2	CELSR3	EIF4A1	GPR156	KDM6B	MT-ND1	PCDHGA5	RET	SPDYE6	WDR87
ARID5A	CHD4	ELF4	GRAF	KIAA0090	MT-ND5	PCDHGB1	RGN	SPPL2C	WFDC12
ARNT	CHD9	EMID1	GRIA2	KIAA0240	MUC12	PCDHGB2	RILP	SRCAP	WHSC1L1
ASAH2B	CHIC2	EML5	GRIA4	KIF26A	MUC16	PCSK2	RIMS2	SRGAP2	WT1
ASB2	CHIT1	EP300	GRK7	KIF26B	MUC4	PDGFR	RNF213	SRMS	XIRP2
ASGR1	CHRNA5	EPHB1	GRM8	KIF7	MUC5AC	PDZD2	RNF24	SRSF2	XKR4
ASTN2	CLMN	EPM2AIP1	GRXCR1	KIT	MUC5B	PEG10	RP1L1	SSH3BP1	XPO7
ASXL1	CLTC	EPOR	GRXCR2	KLHL7	MUC6	PER1	RPL22	STAG2	YLPM1
ASXL2	CNGA4	ETV6	GYG1	KRAS	MYBPHL	PHF6	RPN1	STEAP4	YOD1
ASXL3	CNTNAP4	EVI1	HEAB	LAMA1	MYH11	PHIP	RPS6KA5	STK40	YTHDC1
ATP2A2	CPEB3	EVPLL	HELZ	LAMA3	MYO1D	PHTF1	RTL1	SUPT5H	ZBTB7A
ATP2B2	CREBBP	EXOC6	HERC2	LASP1	MYST4	PIK3CA	RTN1	SUSD2	ZDHHC5
ATP2B3	CRHR1	EZH2	HLXB9	LAT	NAP1L2	PIK3R6	RUNX1	SUV39H2	ZFHX4
ATRX	CRLF2	FACL6	HMCN1	LCX	NAV1	PKD1L2	RUNXBP2	SUV420H1	ZNF16
ATXN3	CRNN	FAM123C	HOXA13	LDB3	NCOA2	PKHD1	RUSC1	SUZ12	ZNF195
AZI1	CSF3	FAM135B	HOXA9	LEF1	NCOA3	PML	RXFP3	SYNGAP1	ZNF275
BAT2	CSMD1	FAM166A	HOXC11	LGALS9	NECAB2	PMX1	RYR3	TCHH	ZNF416
BAT2L2	CSRNP2	FAM57B	HOXC13	LILRA2	NF1	PNUTL1	SAMHD1	TECR	ZNF479
BAZ2B	CT62	FAM5C	HOXD11	LILRA6	NFE2	POLD1	SCAMP3	TESK1	ZNF609
BCORL1	CTCF	FAM65A	HOXD13	LOC64366	NFIB	POLG	SCAMP5	TET1	ZNF79
BMP7	CTNNA2	FAM65B	HP	LPHN3	NFIX	POLL	SCN9A	TET2	ZNF80
BPGM	CWC22	FAT1	HRCT1	LRIT3	NFKBIZ	POTEE	SCUBE1	TET3	ZNF814
BRAT1	CXADR	FAT2	HS6ST1	LRP1B	NLGN3	POU2F2	SEC14L3	TG	ZNF831
BRCA1	CXORF57	FAT3	HTRA1	LRP2	NOTCH1	POU2F3	SEC22B	THG1L	ZRSR2
BRD8	CYP4A11	FAT4	HYAL1	LRRIQ4	NOTCH2	POU4F2	SEMA4G	TIE1	ZXDC

Supplementary Table S2: Antibodies used for flow cytometric analysis

Name	Fluorochrome	Catalog Number	Clone	Supplier
CD117	APC	17-1171-83	2B8	EbioScience
CD117	APC-eFluo780	47-1171-82	2B8	EbioScience
CD11b	PE-Cy7	25-0112-82	M1/70	EbioScience
CD11b	FITC	11-0112-82	M1/70	EbioScience
CD127	AlexaFluor488	53-1271-82	A7R34	EbioScience
CD135	PE	12-1351-83	A2F10	EbioScience
CD16/CD32	Biotin	45-0161-82	93	EbioScience
CD19	PE-Cy7	25-0193-82	eBio1D3	EbioScience
CD24	APC-eFluo780	47-0242-82	M1/69	EbioScience
CD25	AlexaFluor488	53-0251-82	PC61.5	EbioScience
CD34	FITC	11-0341-82	RAM34	EbioScience
CD3e	PE-Cy7	25-0031-82	145-2C11	EbioScience
CD3e	APC	17-0031-83	145-2C11	EbioScience
CD4	APC-eFluo780	47-0041-82	GK1.5	EbioScience
CD43	FITC	561856	S7	BDBioScience
CD44	PE-Cy7	25-0441-82	IM7	EbioScience
CD45.1	APC-eFluo780	47-0453-82	A20	EbioScience
CD45.2	FITC	11-0454-82	Co4	EbioScience
CD45R (B220)	PE-Cy7	25-0452-82	RA3-6B2	EbioScience
CD71	APC	17-0711-82	R17217	EbioScience
CD8a	PE	12-0081-83	53-6.7	EbioScience
F4/80	APC	17-4801-82	BM8	EbioScience
IgM	APC	1020-118		Southern Biotech
Ly-51	PE	553735	BP-1	BDBioScience
Ly6A/E (Sca-1)	PerCP-Cy5.5	45-5981-82	P7	EbioScience
Ly6G (Gr-1)	PE-Cy7	25-5931-82	RB6-8C5	EbioScience
Ly-6G (Gr-1)	PE	12-5931-83	RB6-8C5	EbioScience
TER-119	PE-Cy7	25-5921-82	TER-119	EbioScience